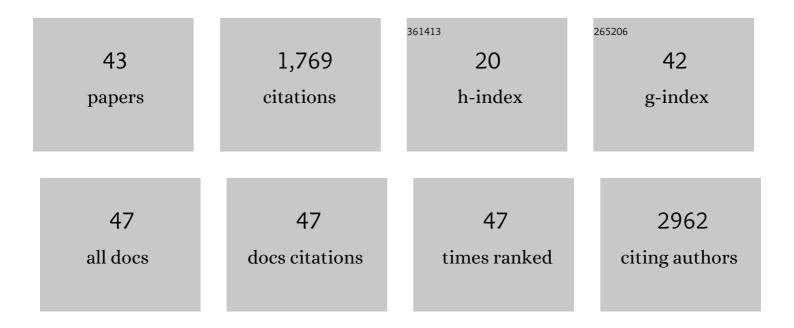
## Stephen P Thompson

List of Publications by Year in descending order

Source: https://exaly.com/author-pdf/2215995/publications.pdf Version: 2024-02-01



#	Article	IF	CITATIONS
1	Multi-stimulus linear negative expansion of a breathing M(O <sub>2</sub> CR) <sub>4</sub> -node MOF. Faraday Discussions, 2021, 225, 133-151.	3.2	2
2	Laboratory exploration of mineral precipitates from Europa's subsurface ocean. Journal of Applied Crystallography, 2021, 54, 1455-1479.	4.5	1
3	Long-Term Stability of MFM-300(Al) toward Toxic Air Pollutants. ACS Applied Materials & Interfaces, 2020, 12, 42949-42954.	8.0	19
4	Mapping the structural transitions controlled by the trilinear coupling in Ca3-xSrxTi2O7. Journal of Applied Physics, 2019, 125, 244102.	2.5	11
5	Effects of quenching on phase transformations and ferroelectric properties of 0.35BCZT-0.65KBT ceramics. Journal of the European Ceramic Society, 2019, 39, 4070-4084.	5.7	10
6	Crystallisation of amorphous Mg-Fe silicates produced from microwave-dried sol-gels. Proceedings of the International Astronomical Union, 2019, 15, 408-409.	0.0	0
7	X-ray powder diffraction study of the stability of clathrate hydrates in the presence of salts with relevance to the Martian cryosphere. Geochimica Et Cosmochimica Acta, 2019, 245, 304-315.	3.9	1
8	A slow-cooling-ratein situcell for long-duration studies of mineral precipitation in cold aqueous environments on Earth and other planetary bodies. Journal of Applied Crystallography, 2018, 51, 1197-1210.	4.5	1
9	Solvent-switchable continuous-breathing behaviour in a diamondoid metal–organic framework and its influence on CO2 versus CH4 selectivity. Nature Chemistry, 2017, 9, 882-889.	13.6	293
10	New synchrotron powder diffraction facility for long-duration experiments. Journal of Applied Crystallography, 2017, 50, 172-183.	4.5	35
11	Amorphous silicate nanoparticles with controlled Fe-Mg pyroxene compositions. Journal of Non-Crystalline Solids, 2016, 447, 255-261.	3.1	4
12	Cation Control of Molecular Sieving by Flexible Li-Containing Zeolite Rho. Journal of Physical Chemistry C, 2016, 120, 19652-19662.	3.1	45
13	Exploration of a potential difluoromethyl-nucleoside substrate with the fluorinase enzyme. Bioorganic Chemistry, 2016, 64, 37-41.	4.1	20
14	Enzymatic transhalogenation of dendritic RGD peptide constructs with the fluorinase. Organic and Biomolecular Chemistry, 2016, 14, 3120-3129.	2.8	13
15	In situ apparatus for the study of clathrate hydrates relevant to solar system bodies using synchrotron X-ray diffraction and Raman spectroscopy. Astronomy and Astrophysics, 2015, 574, A91.	5.1	5
16	Phase space investigation of the lithium amide halides. Journal of Alloys and Compounds, 2015, 645, S343-S346.	5.5	2
17	Dynamic strain propagation in nanoparticulate zirconia refractory. Journal of Applied Crystallography, 2015, 48, 386-392.	4.5	1
18	Structural changes of synthetic paulingite (Na,H-ECR-18) upon dehydration and CO <sub>2</sub> adsorption. Zeitschrift Fur Kristallographie - Crystalline Materials, 2015, 230, 223-231.	0.8	13

#	Article	IF	CITATIONS
19	Cation Gating and Relocation during the Highly Selective "Trapdoor―Adsorption of CO <sub>2</sub> on Univalent Cation Forms of Zeolite Rho. Chemistry of Materials, 2014, 26, 2052-2061.	6.7	96
20	A Localized Tolerance in the Substrate Specificity of the Fluorinase Enzyme enables "Last‣tep― <sup>18</sup> Fâ€Fluorination of a RGD Peptide under Ambient Aqueous Conditions. Angewandte Chemie - International Edition, 2014, 53, 8913-8918.	13.8	48
21	Thermal breakdown of calcium carbonate and constraints on its use as a biomarker. Icarus, 2014, 229, 1-10.	2.5	11
22	Re-entrant structural phase transition in a frustrated kagome magnet, Rb2SnCu3F12. CrystEngComm, 2013, 15, 7426.	2.6	10
23	Zipping and Unzipping of a Paddlewheel Metal–Organic Framework to Enable Twoâ€&tep Synthetic and Structural Transformation. Chemistry - A European Journal, 2013, 19, 3552-3557.	3.3	28
24	Experimental and DFT-D Studies of the Molecular Organic Energetic Material RDX. Journal of Physical Chemistry C, 2013, 117, 8062-8071.	3.1	56
25	Elucidating the Breathing of the Metal–Organic Framework MIL-53(Sc) with ab Initio Molecular Dynamics Simulations and in Situ X-ray Powder Diffraction Experiments. Journal of the American Chemical Society, 2013, 135, 15763-15773.	13.7	173
26	Thermal processing and crystallization of amorphous Mg a silicates. Meteoritics and Planetary Science, 2013, 48, 1459-1471.	1.6	7
27	A novel structural form of MIL-53 observed for the scandium analogue and its response to temperature variation and CO <sub>2</sub> adsorption. Dalton Transactions, 2012, 41, 3937-3941.	3.3	95
28	Fine-grained amorphous calcium silicate CaSiO3 from vacuum dried sol–gel – Production, characterisation and thermal behaviour. Journal of Non-Crystalline Solids, 2012, 358, 885-892.	3.1	24
29	Understanding Carbon Dioxide Adsorption on Univalent Cation Forms of the Flexible Zeolite Rho at Conditions Relevant to Carbon Capture from Flue Gases. Journal of the American Chemical Society, 2012, 134, 17628-17642.	13.7	158
30	New Twists on the Perovskite Theme: Crystal Structures of the Elusive Phases R and S of NaNbO <sub>3</sub> . Inorganic Chemistry, 2012, 51, 6876-6889.	4.0	78
31	Structural Phase Transition in theS=1/2Kagome System Cs2ZrCu3F12and a Comparison to the Valence-Bond-Solid Phase in Rb2SnCu3F12. Chemistry of Materials, 2011, 23, 4234-4240.	6.7	18
32	Structural Chemistry, Monoclinic-to-Orthorhombic Phase Transition, and CO <sub>2</sub> Adsorption Behavior of the Small Pore Scandium Terephthalate, Sc <sub>2</sub> (O <sub>2</sub> CC <sub>6</sub> H <sub>4</sub> CO <sub>2</sub> ) <sub>3</sub> , and Its Nitro- And Amino-Functionalized Derivatives. Inorganic Chemistry, 2011, 50, 10844-10858.	4.0	75
33	A co-templating route to the synthesis of Cu SAPO STA-7, giving an active catalyst for the selective catalytic reduction of NO. Microporous and Mesoporous Materials, 2011, 146, 36-47.	4.4	44
34	High-throughput powder diffraction on beamline I11 at Diamond. Journal of Applied Crystallography, 2011, 44, 102-110.	4.5	28
35	Fast X-ray powder diffraction on I11 at Diamond. Journal of Synchrotron Radiation, 2011, 18, 637-648.	2.4	108
36	Synthesis and structural characterisation using Rietveld and pair distribution function analysis of layered mixed titanium–zirconium phosphates. Journal of Solid State Chemistry, 2010, 183, 2196-2204.	2.9	9

#	Article	IF	CITATIONS
37	Molecular Modeling, Multinuclear NMR, and Diffraction Studies in the Templated Synthesis and Characterization of the Aluminophosphate Molecular Sieve STA-2. Journal of Physical Chemistry C, 2010, 114, 12698-12710.	3.1	44
38	Novel Large-Pore Aluminophosphate Molecular Sieve STA-15 Prepared Using the Tetrapropylammonium Cation As a Structure Directing Agent. Chemistry of Materials, 2010, 22, 338-346.	6.7	35
39	High-Throughput Continuous Hydrothermal Synthesis of an Entire Nanoceramic Phase Diagram. ACS Combinatorial Science, 2009, 11, 829-834.	3.3	65
40	High-performance X-ray detectors for the new powder diffraction beamline I11 at Diamond. Journal of Synchrotron Radiation, 2008, 15, 43-49.	2.4	29
41	Crystallisation processes in cosmic silicates: Laboratory progress towards understanding structural–spectral relationships. Advances in Space Research, 2007, 39, 375-391.	2.6	9
42	The role of residual stress in the fracture properties of a natural ceramic. Journal of Materials Chemistry, 2005, 15, 947.	6.7	18
43	Software for automatic calibration of synchrotron powder diffractometers. Journal of Synchrotron Radiation, 2003, 10, 183-186.	2.4	9